

# A Precise Charge Balancing and Compliance Voltage Monitoring Stimulator Front-End for 1024-electrodes Retinal Prosthesis

Hosung Chun, Nhan Tran, Yuanyuan Yang, Omid Kavehei, Shun Bai and Stan Skafidas  
Department of Electrical and Electronic Engineering, University of Melbourne  
Melbourne, Australia  
Email: hosung.chun@unimelb.edu.au

**Abstract**—In this paper, we present a precise charge balancing and compliance voltage monitoring stimulator front-end for 1024-electrode retinal prosthesis. Our stimulator is based on current mode stimulation. To generate a precisely matched biphasic current pulse, a dynamic current copying technique is applied at the stimulator front-end. A compliance voltage monitoring circuitry is included at the stimulator front-end to detect if a voltage across electrode-tissue interface goes beyond a predefined compliance voltage. Simulation results show the mismatch of a biphasic current pulse (at a maximum stimulation current of  $476\mu\text{A}$ ) is less than 0.1%. Also, the stimulator issues alarm signals, when a voltage compliance occurs during stimulation due to high tissue impedance. Our stimulator is implemented using a 65nm low voltage (LV) CMOS process, which helps reducing implementation area and power consumption.

## I. INTRODUCTION

To restore vision to the blind, who suffered from retinal diseases, such as retinitis pigmentosa (RP) and age-related macular degeneration (AMD), vision prostheses have been developed over the past decades [1], [2] and [3]. It is reported that several hundreds electrodes (even up to 1000) will be needed to restore useful vision to the blind, so that the blind can read letters, navigate a room and recognise faces [4]. As interfacing a retina with penetrating electrodes requires less charge threshold to induce a sense of light (phosphene) from the blind [5], it is feasible to implement a stimulator with LV CMOS process. So we aim to implement a vision prosthesis with 1024-electrode array using a 65nm LV CMOS process. This reduces implementation area and power consumption of the stimulator significantly.

Our stimulator is based on the current mode stimulation, employing a typical biphasic current pulse, due to easy control of injecting charge into the retinal tissue. To ensure safety in the current mode stimulation, it is necessary to guarantee zero-net charge transfer (perfect charge balance) into nerve cells during electrical stimulation, which prevents DC current flowing into tissue. This necessitates a perfectly matched biphasic current pulse, which ideally ensures no residual charge on a stimulating electrode pair (preventing DC current flowing into tissue) after stimulation. During electrical stimulation, a large voltage excursion occurs at electrode-tissue interface due to high tissue impedance. For a desired stimulation, the voltage across electrode-tissue interface should remain in a predefined voltage compliance limit, so that current drivers can keep a voltage headroom.

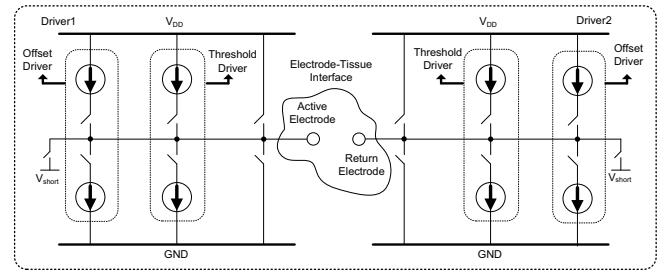


Fig. 1. Previous Stimulator Front-End Architecture

Otherwise, current drivers may produce unmatched biphasic current pulses, leading to possible tissue damage.

Therefore, in this paper, we present a stimulator front-end with safety enhanced features; precise charge balance and compliance voltage monitor. For this aim, a dynamic current copying [6] and compliance voltage monitoring circuits are applied at the stimulator front-end. This paper is organised as follows. Previous stimulator architecture is discussed in Section II. Section III presents safety enhanced features; precise charge balance and voltage compliance monitor. Circuit implementation is in Section IV. Section V shows simulation results. Conclusion is drawn in Section VI.

## II. PREVIOUS STIMULATOR ARCHITECTURE

We aim to implement a vision prosthesis with 1024 electrodes with 1024 drivers. In other words, each electrode has its own dedicated driver, which can connect the electrode to either a current sink or a current source or  $V_{DD}$  or GND or a shorting potential, according to stimulation profile [7], [8]. This is illustrated in Fig.1. During a cathodic phase, an active (working) electrode is firstly connected to a current sink of either a threshold driver or an offset driver or both, while a return (counter) electrode is pulled up to  $V_{DD}$ . In the following phase (anodic), the active electrode is connected to a current source of either a threshold driver or an offset driver or both, while the return electrode is pulled down to GND. This structure requires less voltage headroom, as only one current sink or source is activated during stimulation. Therefore, this gives more voltage compliance.

Each driver consists of two independent drivers; a threshold driver and an offset driver. Each provides 32 different current levels. The threshold driver is utilised to find out a minimum threshold current to induce phosphene. Threshold current may be different at each driver, as different regions of the

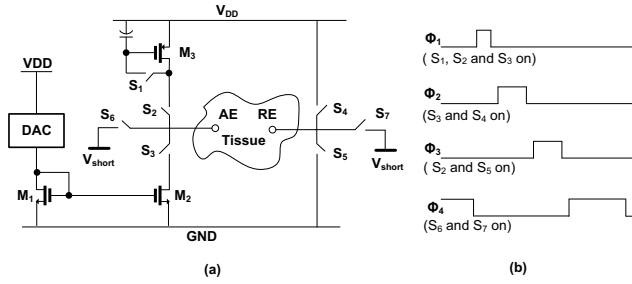


Fig. 2. (a) Concept of Dynamic Current Copying and (b) Operating Sequence

retinal surface require different thresholds. Once phosphene is detected, the output of the threshold driver is fixed at the minimum threshold current. Then, further increase on the stimulation current is provided by the offset driver. The details of our previous implementation are well addressed in [7], [8].

### III. CURRENT ARCHITECTURE WITH ENHANCED SAFETY

#### A. Precise Charge Balance

Electrical stimulation performed with unmatched biphasic current pulses is likely to damage tissue, due to DC current flowing into tissue. Therefore, for safety, it is necessary to carry out stimulation with precisely matched biphasic current pulses. In practice, due to CMOS process imperfection, it is difficult to implement a stimulator, which can generate a perfectly matched biphasic current pulse. However, employing dynamic current copying technique at a stimulator front-end improves a matching accuracy of a biphasic current pulse to the extent of preventing tissue damage, without any area and power penalties [6]. Therefore, we apply this technique at the stimulator front-end for our high density retinal prosthesis with 1024-electrode array.

The brief concept of the stimulator front-end with dynamic current copying is illustrated in Fig.2, where AE and RE is an active electrode and a return electrode, respectively. Basically, it operates in 4 sequences for single stimulation. During  $\Phi_1$  (sampling phase),  $S_1$ ,  $S_2$  and  $S_3$  are closed. The current from the DAC is reproduced at  $M_2$  and  $M_3$ .  $M_3$  stores its gate source voltage in the capacitor. In  $\Phi_2$  (cathodic phase),  $S_3$  and  $S_4$  are on. Then, cathodic current flows from  $V_{DD}$  to  $M_2$  via RE and AE. Anodic current flows from  $M_3$  to GND via AE and RE, while  $S_2$  and  $S_5$  are on during  $\Phi_3$  (anodic phase). During  $\Phi_4$  (shorting), AE and RE are connected to a shorting potential by closing  $S_6$  and  $S_7$ .

#### B. Compliance Voltage Monitor

In current mode stimulation, a current source (made of PMOS transistors) and a current sink (made of NMOS transistors) need a minimum voltage headroom, which puts PMOS and NMOS transistors in saturation mode, so that they can work as a constant current source and sink during stimulation. A voltage compliance is defined as an available voltage across electrode-tissue interface during stimulation. In other words, it is a remaining voltage after deducting this

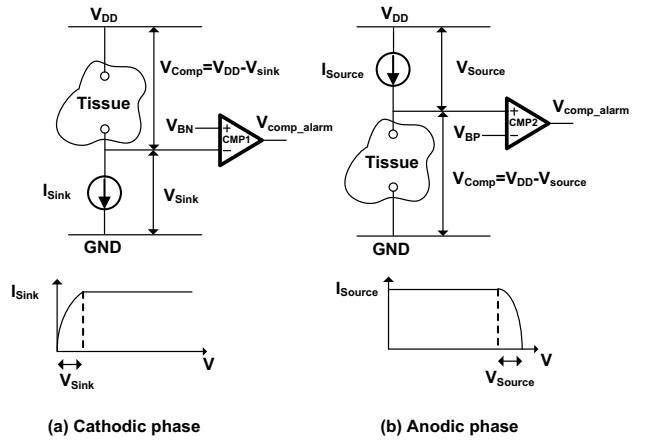


Fig. 3. Voltage Compliance (a) During Cathodic Phase and (b) During Anodic Phase

minimum voltage headroom from supply voltage. This is illustrated in Fig.3. For a desired stimulation, it is important to ensure that a voltage across electrode-tissue interface always remains within a voltage compliance. Once the voltage across the electrode-tissue interface goes over the predefined voltage compliance due to high tissue impedance, either a current source or sink will stop working as a constant current source or sink. Consequently, it is not possible to generate a precisely matched biphasic current pulse.

In Fig.3, a compliance voltage monitoring circuit is implemented with CMP1 and CMP2.  $V_{BP}$  and  $V_{BN}$  are predefined values and set the voltage headroom for a current source and sink, respectively. The detailed operation is discussed in the next section.

### IV. CIRCUIT IMPLEMENTATION

Fig.4 shows a complete schematic of the implemented stimulator front-end. Supply voltage ( $V_{DD}$ ) is 3.3V. An active cascode structure is utilised for current source and sink drivers to reduce the channel length modulation effect in a given process.

#### A. Dynamic Current Copying at Stimulator Front-End

A current source driver consists of  $M_{OP}$ ,  $M_{C2}$ ,  $C_1$  and  $OTA_2$ . A threshold DAC and an offset DAC are combined to form a current sink driver, cascoded with  $M_{C1}$  and  $OTA_1$ . A 5 bit binary-weighted current DAC is utilised for these DACs. The threshold DAC is utilised to search a minimum threshold current to induce phosphene. Once phosphene is detected, the code word of the threshold DAC is saved. Then, further increase on the stimulation current is added by the offset DAC. The threshold/offset DAC's current is copied from the DAC1/DAC2, which is a 4 bit DAC with LSB current of  $0.5\mu A$ . With this structure, a stimulator can provide wide range stimulation currents with different step sizes. For instance, by setting DAC1's output at  $5\mu A$ , the threshold DAC's output currents range from  $5\mu A$  to  $155\mu A$ , with a step of  $5\mu A$ . If the output of DAC2 is  $2\mu A$ , the offset DAC's currents will vary between  $2\mu A$  and  $62\mu A$ , with a step

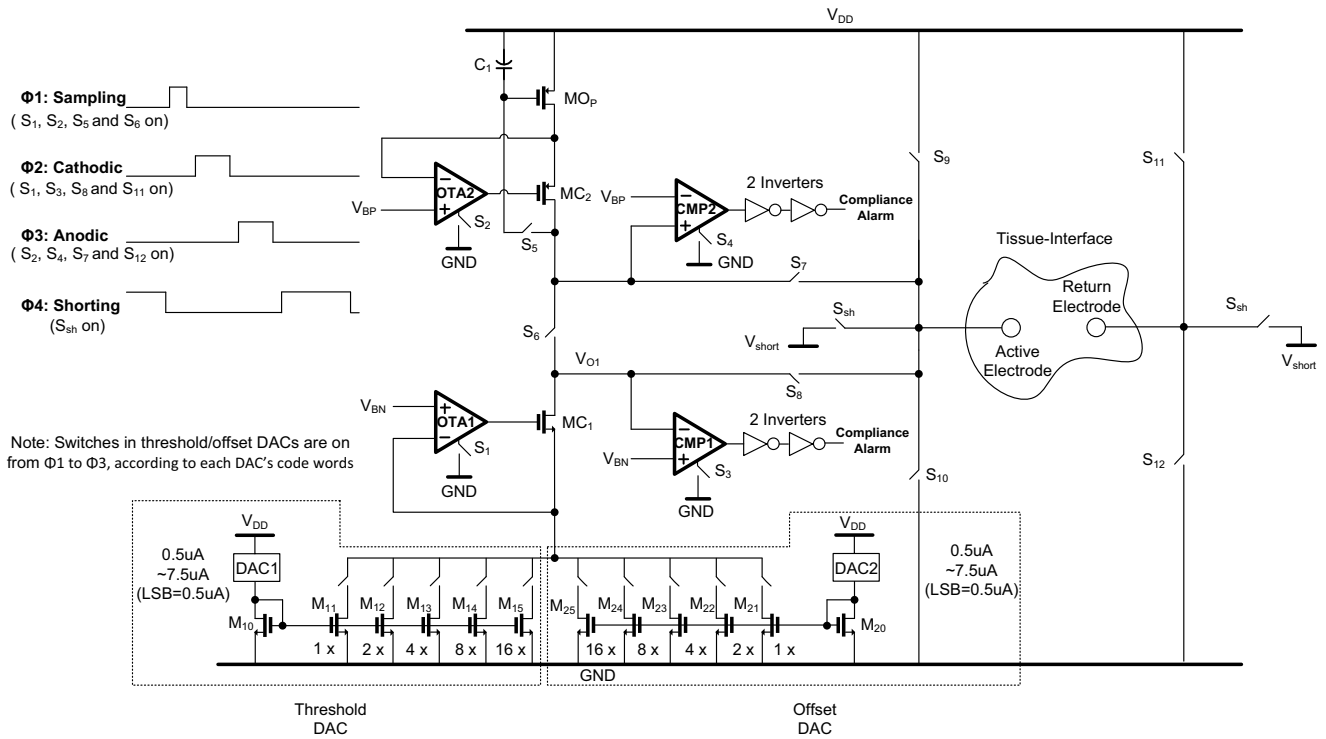


Fig. 4. Complete Schematic of the Stimulator Front-End

of  $2\mu\text{A}$ . A sink current is simply the sum of the threshold and offset DAC's currents.

For OTA1 and OTA2, a PMOS input OTA and an NMOS OTA in [9] are utilised. OTA1 and OTA2 are designed to consume less than  $50\mu\text{W}$  each and their settling time is less than  $1\mu\text{s}$ . The minimum required time for the sampling phase ( $\Phi_1$ ) heavily depends on the settling time of OTA1 and OTA2. To reduce a channel charge injection from  $S_5$  to  $C_1$ , a transmission gate with a dummy structure is used for  $S_5$ . Also, a large capacitor (4pF mimcap) is used for  $C_1$ .

### B. Compliance Voltage Monitor

In Fig.4, CMP1 and CMP2 are included to monitor the voltage headroom of the current source and sink drivers. A PMOS input OTA and an NMOS input OTA in [9] are utilised for CMP1 and CMP2, respectively. A wide transistor ( $200\mu\text{m}/2\mu\text{m}$ ) is used for cascode transistors ( $MC_1$  and  $MC_2$ ), so that the voltage drop across them would be small (tens of mV).  $V_{BN}$  and  $V_{BP}$  are designed to be 0.3V and 3.0V. The voltage compliance during a cathodic and anodic phases becomes 3.0V, out of 3.3V, which is 90% of supply voltage. The voltage headroom for the current sink driver is monitored at  $V_{O1}$  during  $\Phi_2$  (cathodic phase). When the current sink driver works in a normal way,  $V_{O1}$  will be greater than 0.3V. By any chance, if  $V_{O1}$  is below the predefined voltage headroom ( $V_{BN}=0.3\text{V}$ ), the current sink driver goes into triode region, indicating that a voltage across electrode-tissue interface is more than the voltage compliance (3V). Then, CMP1's output goes high and CMP1 issues an alarm signal to a central controller, so that it would stop stimulation

right away. Similarly, CMP2 performs a compliance voltage monitoring during  $\Phi_3$  (anodic phase).

### C. Operating Sequence

During  $\Phi_1$  (sampling phase), a dynamic current copying is carried out by connecting the current source and sink drivers.

In  $\Phi_2$  (cathodic phase), cathodic current flows from  $V_{DD}$  to the current sink driver, while anodic current flows from the current source driver to GND in  $\Phi_3$  (anodic phase). During  $\Phi_4$  (shorting), electrodes are connected to a shorting potential, removing any residual charge on the electrodes.

## V. SIMULATION RESULTS

Simulations are performed with following parameters; 1) stimulation period: 3ms, 2)  $\Phi_1$ :  $50\mu\text{s}$ , 3)  $\Phi_2$ : 1ms, 4)  $\Phi_3$ : 1ms and 5)  $\Phi_4$ : 0.92ms. A minimum time for  $\Phi_1$  is  $10\mu\text{s}$ , which is determined by the settling time of OTAs. Inter-phase delay is set to  $10\mu\text{s}$ . Note that the worst case mismatch of a biphasic curve will occur at a maximum stimulation current, at which the output impedance of current drivers will be minimum. Fig.5 displays generated biphasic current curves with a maximum stimulation current of  $476\mu\text{A}$ . The targeted maximum stimulation current was  $465\mu\text{A}$ , a sum of the maximum threshold DAC current ( $232.5\mu\text{A}$ ) and the maximum offset DAC current ( $232.5\mu\text{A}$ ). However, due to a mismatch in CMOS process, the maximum stimulation current becomes  $476\mu\text{A}$ . The first and third biphasic curves are generated with tissue resistance of  $3\text{k}\Omega$ . The cathodic current is  $476.15\mu\text{A}$ , while the anodic current is  $476.19\mu\text{A}$ . This is less than 0.1% mismatch between the cathodic and anodic currents. No voltage compliance alarm is issued, as

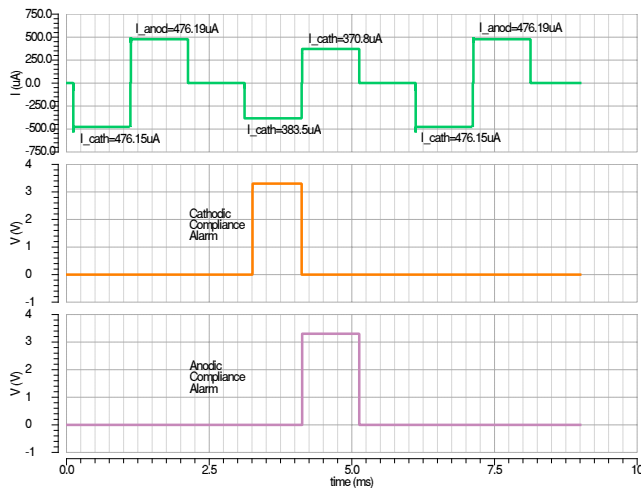


Fig. 5. Simulated Biphasic Current Pulses with Voltage Compliance Alarm

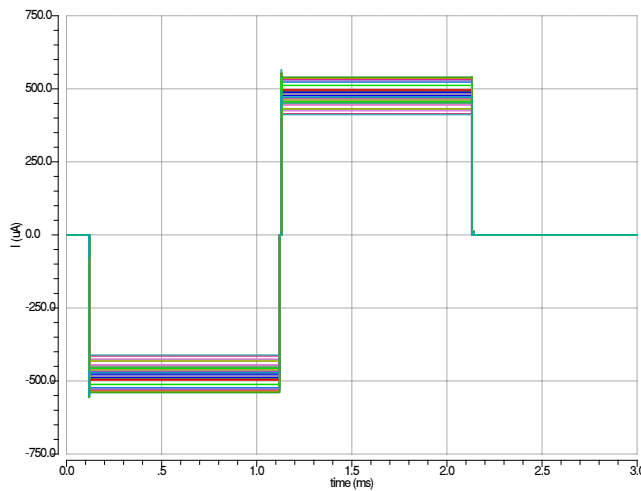


Fig. 6. Monte-Carlo Simulation Results

the voltage across the tissue resistance is around 1.43V, still under the voltage compliance limit (3V). The second biphasic curve is simulated with  $8k\Omega$  tissue resistance. The cathodic current is  $383.5\mu A$  and the anodic current is  $370.8\mu A$ . At this time, the biphasic current pulse is not matched well. When the current drivers try to push (pull) the targeted stimulation current of  $476\mu A$  into (from) the tissue resistance, the voltage across the tissue resistance goes over the voltage compliance limit (3V). Consequently, the minimum voltage headroom for the current drivers is not guaranteed during stimulation, failing to deliver the desired current of  $476\mu A$ . Then, the voltage compliance alarm is issued both at cathodic and anodic phases.

Monte-Carlo simulation is carried out with the maximum stimulation current (shown in Fig.6) and summarised in Table.I. Though the stimulation current varies from  $414\mu A$  to  $542\mu A$  (approximately  $\pm 13\%$  variation from the nominal value of  $476\mu A$ ), the differences between the cathodic current and the anodic current are kept below  $0.3\mu A$ . This is less than 0.1% mismatch.

TABLE I  
MONTE-CARLO SIMULATION RESULTS

	$I_{Cathodic}$	$I_{Anodic}$	$\Delta I$	% error
Min	$413.91\mu A$	$414.12\mu A$	$0.21\mu A$	< 0.1%
Nominal	$476.15\mu A$	$476.19\mu A$	$0.04\mu A$	< 0.1%
Max	$541.78\mu A$	$542.05\mu A$	$0.27\mu A$	< 0.1%

## VI. CONCLUSION

In this paper, we present a precise charge balancing and compliance voltage monitoring stimulator front-end for 1024-electrode retinal prosthesis. To generate a precisely matched biphasic curve, a dynamic current copying is applied at the stimulator front-end. In simulation, the mismatch of a biphasic current pulse (at a maximum stimulation current of  $476\mu A$ ) was less than 0.1%. The voltage compliance monitoring circuitry is also included at the stimulator front-end. It checks if a voltage across electrode-tissue interface during stimulation goes beyond a predefined compliance voltage. If this occurs, it produces an alarm signal to a control unit, so that the stimulation would be stopped right away.

## REFERENCES

- [1] M. Sivaprakasam, W. Liu, G. Wang, J. Weiland, and M. Humayun, "Architecture tradeoffs in high-density microstimulators for retinal prosthesis," *Circuits and Systems I: Regular Papers, IEEE Transactions on*, vol. 52, no. 12, pp. 2629–2641, 2005.
- [2] M. Ortmanns, A. Rocke, M. Gehrke, and H. Tiedtke, "A 232-channel epiretinal stimulator ASIC," *Solid-State Circuits, IEEE Journal of*, vol. 42, no. 12, pp. 2946–2959, 2007.
- [3] K. Chen, Z. Yang, L. Hoang, J. Weiland, M. Humayun, and W. Liu, "An integrated 256-channel epiretinal prosthesis," *Solid-State Circuits, IEEE Journal of*, vol. 45, no. 9, pp. 1946–1956, 2010.
- [4] K. Cha, K. Horch, and R. Normann, "Simulation of a phosphene-based visual field: visual acuity in a pixelized vision system," *Annals of biomedical engineering*, vol. 20, no. 4, pp. 439–449, 1992.
- [5] C. Koch, W. Mokwa, M. Goertz, and P. Walter, "First results of a study on a completely implanted retinal prosthesis in blind humans," in *Sensors, 2008 IEEE*. IEEE, 2008, pp. 1237–1240.
- [6] H. Chun, T. Lehmann, and Y. Yang, "Implantable stimulator for bipolar stimulation without charge balancing circuits," in *Biomedical Circuits and Systems Conference (BioCAS), 2010 IEEE*. IEEE, 2010, pp. 202–205.
- [7] N. Tran, J. Yang, S. Bai, E. Skafidas, I. Mareels, D. Ng, and M. Halpern, "A flexible electrode driver using 65 nm CMOS process for 1024-electrode epi-retinal prosthesis," in *Future Information Technology (FutureTech), 2010 5th International Conference on*. IEEE, 2010, pp. 1–5.
- [8] N. Tran, E. Skafidas, J. Yang, S. Bai, M. Fu, D. Ng, M. Halpern, and I. Mareels, "A prototype 64-electrode stimulator in 65 nm CMOS process towards a high density epi-retinal prosthesis," in *Engineering in Medicine and Biology Society, EMBC, 2011 Annual International Conference of the IEEE*. IEEE, 2011, pp. 6729–6732.
- [9] P. Allen and D. Holberg, "CMOS analog circuit design," 2002.